

Magnetocrystalline Energy, Electronic Charge Distribution, and Fermi Surface of Iron from a Tight-Binding Calculation

M. ASDENTE

Laboratori Centro Informazioni Studi Esperienze-Segrate, Milan, Italy, and Politecnico di Milano, Milan, Italy

AND

M. DELITALA*

Istituto di Fisica dell'Università, Parma, Italy

(Received 17 March 1967)

By introducing the spin-orbit coupling, the first constant K_1 of the magnetocrystalline energy of bcc Fe has been evaluated, using 284 nonequivalent points of the Brillouin zone. Previous results obtained with the tight-binding approximation are used. K_1 is found to be positive, in agreement with the experimental data on the directions of easy magnetization, but its value is lower than expected. The $3d$ -electron charge distributions for the t_{2g} and e_g symmetries are given as a function of energy. Both the charge and spin densities show the same kind of deviation from spherical symmetry as the ones deduced, respectively, by x-ray and neutron-diffraction experimental results. Finally, the shape of Fermi surface in paramagnetic and ferromagnetic bcc Fe is suggested.

INTRODUCTION

MUCH attention has been devoted in the last few years to the electronic structure of transition metals both from the experimental and theoretical points of view (see, for instance, articles by Herring¹ and Mott²). It is possible to differentiate two currents of thought regarding the study of d electrons in transition metals: the localized model and the itinerant one. Besides having a more satisfactory mathematical basis, the itinerant model has recently been supported by experimental results concerning galvanomagnetic properties at high fields (for instance, the Hall effect and magnetoresistivity in Fe and Ni³). Thus, the study based on itinerant models has been developed further, a certain number of calculations with different approximations having been performed.

A comparison between different results,^{2,4} both theoretical and experimental, suggests that some general features of density-of-states curves and of electronic eigenfunctions can be found with the tight-binding method, the overlap integrals being treated as parameters or calculated using suitable atomic eigenfunctions and potentials. The main limitation of this method is that it does not include *a priori* the s - d hybridization, as other methods, the augmented-

plane-wave method (APW) for instance, automatically do. Such a limitation may be less catastrophic than expected in the study of certain properties; moreover, for a ferromagnetic metal, it may even prove to be a more suitable approach, as it allows the s and d states to be treated differently as regards exchange energy.² For the d band, the exchange energy is generally represented by an additional contribution $\pm\delta$, depending on the direction of the electron spin; but to assign the same shift to the $4s$ band might not be a good approximation.⁵ In addition, it must be observed that while the general trend of the various $E(\mathbf{k})$ bands is rather insensitive to the details of the potential (always arbitrary to some extent), the relative position of the s and d bands, and consequently the s - d mixing, is drastically affected by them. This necessitates caution in drawing conclusions about properties which are very sensitive to the details of the $E(\mathbf{k})$ curves (such as the form of the Fermi surface), even from very complete and accurate calculations.

In a previous paper⁶ the electron energy $E(\mathbf{k})$ was given as determined from the tight-binding method; the density-of-state curve and the influence of the spin-orbit coupling on $E(\mathbf{k})$ were subsequently determined.

Some results are presented below on other properties of Fe deduced with the same approximations. The first section concerns the evaluation of the first constant of the magnetocrystalline energy. The second is devoted to the asphericity of the $3d$ -electron distribution. Finally, in the third some considerations are presented on the Fermi surface.

* This research has been sponsored in part by the Gruppo Nazionale di Struttura della Materia of the Consiglio Nazionale delle Ricerche.

¹ C. Herring, J. Appl. Phys. **31**, 3S (1960).

² N. F. Mott, Advan. Phys. **13**, 325 (1964).

³ W. A. Reed and E. Fawcett, Phys. Rev. **136**, A422 (1964).
W. A. Reed and E. Fawcett, in *Proceedings of the International Conference on Magnetism, Nottingham, 1964* (The Institute of Physics and The Physical Society, London, 1965), p. 120; A. V. Gold, *ibid.*, p. 124; Phys. Rev. Letters **10**, 227 (1963).

⁴ J. H. Wood, Phys. Rev. **117**, 714 (1960); E. F. Belding, Phil. Mag. **4**, 1145 (1959); F. Stern, Phys. Rev. **116**, 1399 (1959); M. Asdente and J. Friedel, *ibid.* **124**, 384 (1961); **126**, 2262 (*E*) (1962).

⁵ This fact has been confirmed by recent more elaborate calculations. See S. Wakoh and J. Yamashita, J. Phys. Soc. Japan **21**, 1712 (1966); J. Yamashita, S. Wakoh, and S. Asano, in *Quantum Theory of Atoms, Molecules, Solid State*, p. 497 (unpublished).

⁶ E. Abate and M. Asdente, Phys. Rev. **140**, A1303 (1965).

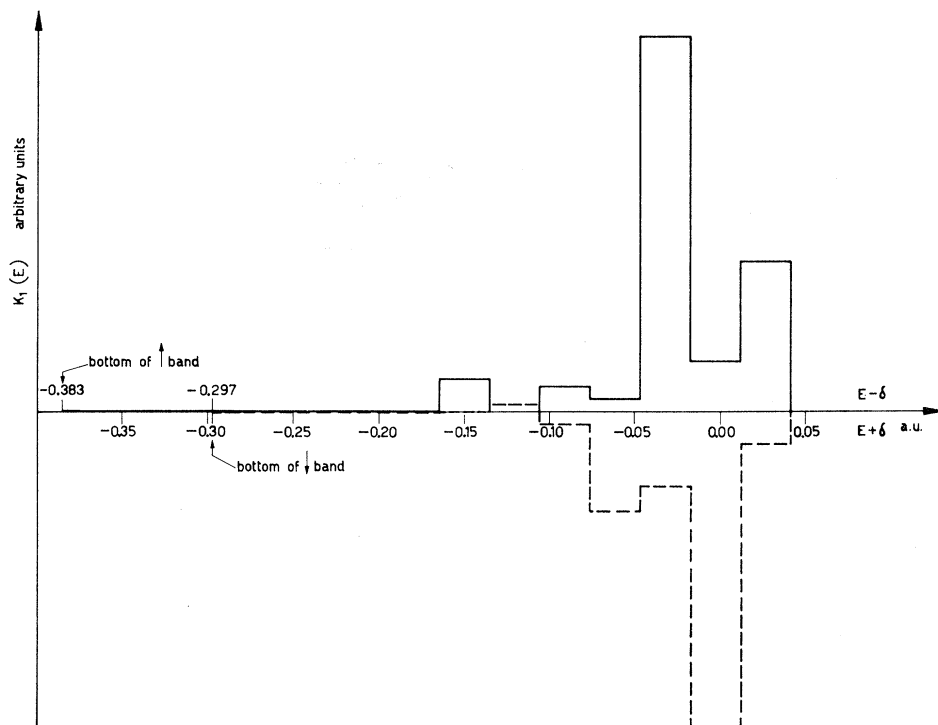


FIG. 1. $K_1(E)$ for the occupied levels of spin-up (full line) and of spin-down (dashed line). The histogram is derived from 284 nonequivalent points of Brillouin zone.

1. THE FIRST CONSTANT OF MAGNETO-CRYSTALLINE ENERGY

It is well known that the free energy of a cubic ferromagnetic crystal has the form

$$E = E_0 + K_1(\alpha_1^2\alpha_2^2 + \alpha_2^2\alpha_3^2 + \alpha_3^2\alpha_1^2) + K_2\alpha_1^2\alpha_2^2\alpha_3^2 + \dots,$$

where K_1 and K_2 are the first and the second constants of anisotropy, and $\alpha_1, \alpha_2, \alpha_3$ are the direction cosines of the magnetization vector with respect to the crystal axis. K_1 is positive for bcc Fe, in agreement with the fact that the direction of easy magnetization is $[100]$.⁷

Obviously, a complete explanation of the origin of the magnetocrystalline energy is subordinate to a theory of ferromagnetism in transition metals, the approach to which is still controversial. Bloch and Gentile⁸ suggested that the spin-orbit interaction can account for the observed coupling between the atomic spin and the crystal axes. In this hypothesis, a tight-binding calculation, including a spin-orbit interaction, allows an evaluation of the constant K_1 to be obtained rather easily.

A first approach in this direction was made by Brooks⁹ for Fe and Ni by considering only three d bands and introducing some quite drastic approximations about

the electronic eigenfunctions and eigenvalues. Subsequently, Fletcher¹⁰ made a similar calculation on Ni, improving the approximations of Brooks's paper and formally extending his theory to a complete d band.

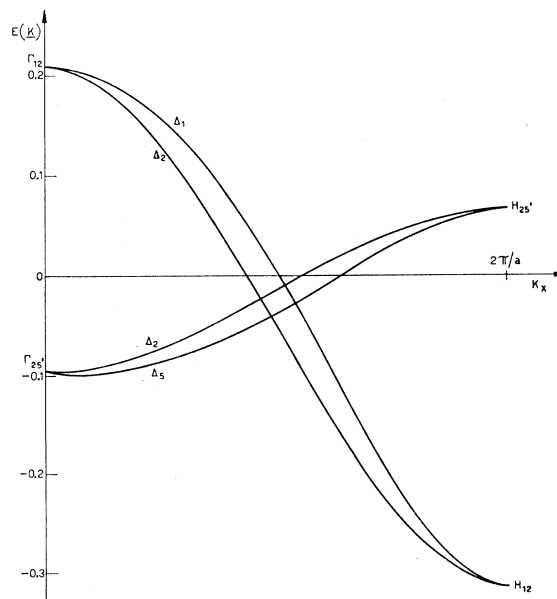


FIG. 2. Energy bands $E(\mathbf{k})$ along the ΓH line (Ref. 6). Energy is in atomic units. Notation of L. P. Bouckaert, R. Smoluchowsky, and E. Wigner, Phys. Rev. **50**, 58 (1936).

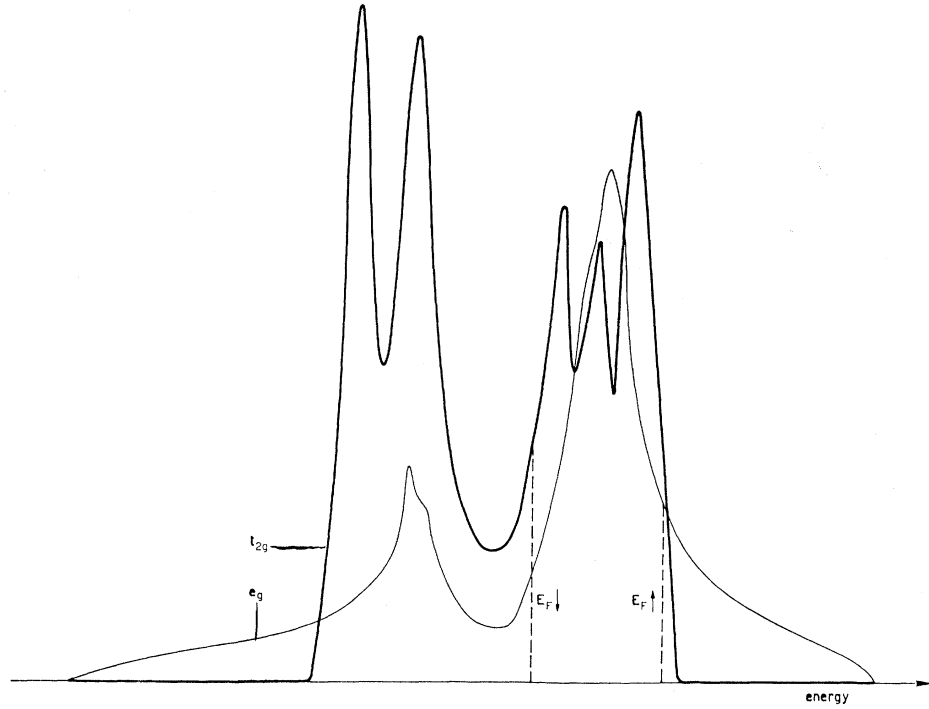
⁷ See, for example, R. M. Bozorth, *Ferromagnetism* (D. Van Nostrand Company, Inc., London, 1951).

⁸ F. Bloch and G. Gentile, Z. Physik **70**, 395 (1931).

⁹ H. Brooks, Phys. Rev. **58**, 909 (1940).

¹⁰ G. C. Fletcher Proc. Phys. Soc. (London) **67**, 505 (1954).

FIG. 3. On the ordinate, the functions $q_{e\uparrow}(E)$, $q_{e\downarrow}(E)$ are represented in arbitrary units. $E_{F\uparrow}$ and $E_{F\downarrow}$ are the spin-up and spin-down Fermi levels in the ferromagnetic state.



We have now considered all five bands for bcc Fe with the approximations outlined in the introduction. The spin-orbit interaction is treated as a perturbation, as compared with the effects of the crystal field and the exchange energy. The matrix elements of the spin-orbit interaction operator with respect to the unperturbed wave functions Ψ_{ik} are deduced by the matrix elements relative to the Bloch functions Φ_{rk} ($\Psi_{ik} = \sum_r a_{ir} \Phi_{rk}$; see also Table II, Ref. 6).

The average contribution to K_1 from 48 equivalent levels in the Brillouin zone is obtained by applying lattice symmetry operations; it appears that, because of cubic symmetry, the fourth-order energy correction is the first to show anisotropy.

The value of K_1 has been obtained by summing the average contribution per level over the occupied levels of the Fermi distribution, excluding the degenerate ones.

The resulting formula is

$$\begin{aligned}
 K_1 &= \frac{1}{3} N \left(\frac{1}{2} \bar{\xi}\right)^4 \sum_{i \text{ occ}} K_{1i}(E_i) \\
 &= \frac{1}{3} N \left(\frac{1}{2} \bar{\xi}\right)^4 \sum_{i \text{ occ}} \left\{ \sum_{\tau, \tau'' \neq i} [-K_{i\tau, \tau\tau', \tau''\tau'', \tau''i}]_{\tau'=i} \right. \\
 &\quad \times (\epsilon_{\tau}^{-1} - [\epsilon_{\tau} + 2\delta(j)]^{-1}) (\epsilon_{\tau''}^{-1} - [\epsilon_{\tau''} + 2\delta(j)]^{-1}) \\
 &\quad \times (\epsilon_{\tau}^{-1} + [\epsilon_{\tau} + 2\delta(j)]^{-1} + [2\delta(j)]^{-1}) \\
 &\quad + \sum_{\tau, \tau', \tau'' \neq i} K_{i\tau, \tau\tau', \tau''\tau'', \tau''i} (\epsilon_{\tau}^{-1} - [\epsilon_{\tau} + 2\delta(j)]^{-1}) \\
 &\quad \left. \times (\epsilon_{\tau'}^{-1} - [\epsilon_{\tau'} + 2\delta(j)]^{-1}) (\epsilon_{\tau''}^{-1} - [\epsilon_{\tau''} + 2\delta(j)]^{-1}) \right\},
 \end{aligned}$$

with

$$i, \tau, \tau', \tau'' = 1, 2, \dots, 5,$$

$$j = 1, 2;$$

$$\delta(1) = -\delta,$$

$$\delta(2) = +\delta;$$

$$\epsilon_{\tau} = E_i - E_{\tau}, \quad \epsilon_{\tau'} = E_i - E_{\tau'}, \quad \text{etc.}$$

$$\begin{aligned}
 K_{i\tau, \tau\tau', \tau''\tau'', \tau''i} &= -5N_{i\tau, \tau\tau', \tau''\tau'', \tau''i} + M_{i\tau, \tau\tau'} M_{\tau''\tau'', \tau''i} \\
 &\quad + M_{i\tau, \tau'\tau''} M_{\tau\tau', \tau''i} + M_{i\tau, \tau''i} M_{\tau\tau', \tau''\tau''},
 \end{aligned}$$

$$\begin{aligned}
 N_{i\tau, \tau\tau', \tau''\tau'', \tau''i} &= A_{i\tau} A_{\tau\tau'} A_{\tau''\tau''} A_{\tau''i} + B_{i\tau} B_{\tau\tau'} B_{\tau''\tau''} B_{\tau''i} \\
 &\quad + C_{i\tau} C_{\tau\tau'} C_{\tau''\tau''} C_{\tau''i};
 \end{aligned}$$

$$M_{i\tau, \tau\tau'} = A_{i\tau} A_{\tau\tau'} + B_{i\tau} B_{\tau\tau'} + C_{i\tau} C_{\tau\tau'},$$

$$A_{i\tau} = (a_{i2} a_{\tau 3} - a_{i3} a_{\tau 2}) + 2(a_{i1} a_{\tau 4} - a_{i4} a_{\tau 1}),$$

$$B_{i\tau} = -(a_{i2} a_{\tau 1} - a_{i1} a_{\tau 2}) - (a_{i3} a_{\tau 4} - a_{i4} a_{\tau 3})$$

$$+ \sqrt{3}(a_{i3} a_{\tau 5} - a_{i5} a_{\tau 3}),$$

$$C_{i\tau} = -(a_{i2} a_{\tau 4} - a_{i4} a_{\tau 2}) - \sqrt{3}(a_{i2} a_{\tau 5} - a_{i5} a_{\tau 2})$$

$$+ (a_{i3} a_{\tau 1} - a_{i1} a_{\tau 3}).$$

N is the number of atoms per cm^3 , $\bar{\xi}$ is the spin-orbit interaction parameter which corresponds to the a_i in the Goudsmit notation,¹¹ and $a_{i\tau}$ and E_i are, respectively, the eigenvectors and the eigenvalues of the unperturbed state. It has been assumed that $\bar{\xi} = 0.0016$

¹¹S. Goudsmit, Phys. Rev. 31, 946 (1928).

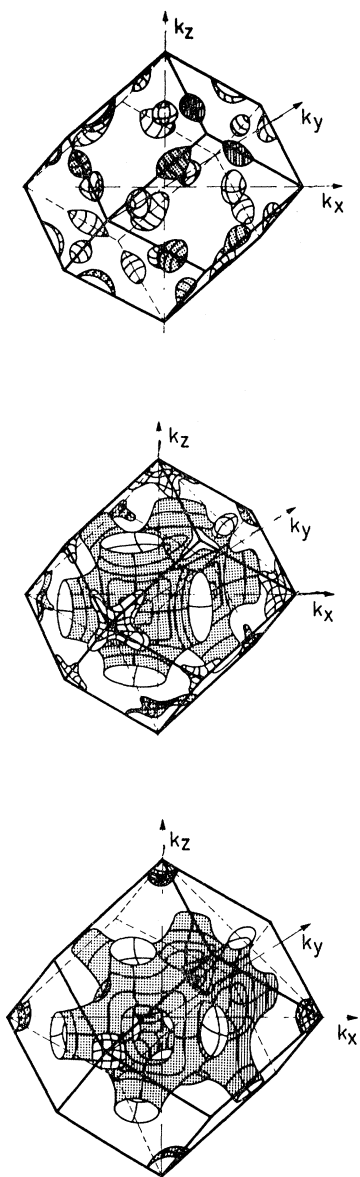


FIG. 4. Fermi surfaces for paramagnetic bcc Fe; the lower figure is for the third zone, the middle one for the fourth zone, and the upper one for the fifth zone. The dark portions of the surfaces are directed towards the occupied states.

a.u., according to spectroscopic data¹²; and $\delta=0.043$ a.u., according to the calculated density-of-state curve and the magnetization value.

The contribution to K_1 from the various levels as a function of the energy of the levels themselves,

$$K_1(E) = \sum_{E < E_i < E + dE} K_{1i}(E_i),$$

has been evaluated step by step, separately for the two spin directions; the result is given in the histogram

¹² E. Moore, *Atomic Energy Levels*, Natl. Bur. Std. (U.S.) Circ. No. 467 (U.S. Government Printing Office, Washington, D.C., 1949).

of Fig. 1, where we have assumed $dE = \text{bandwidth}/20$. It can be seen that the electrons of the two sub-bands generally give average contributions of opposite sign to K_1 . It can also be noted that the levels in the lower half of the band give a negligible contribution compared to that due to the ones in the upper half. A difference between levels at the bottom and at the top of the band has already been noticed in that the eigenfunctions present a bonding and an antibonding character, respectively [M. Asdente and J. Friedel, (Ref. 4)]; these two facts can perhaps be connected.

This calculation was performed with an IBM 7040 computer, and the result was obtained using 284 non-

TABLE I. Values of $3d$ bandwidths and of the exchange splitting ΔE , as calculated by different techniques, from several authors. ΔE is the energy difference between the single-particle energy levels corresponding to + and - spin.

		Width of $3d$ band for iron (eV)
Belding ^a		~5
Wohlfarth ^b		~6.8
Mattheiss ^c		~4
Stern ^a		~9.3
Callaway ^d		~1.6
Wood ^a		6.3-12
Manning ^e		~8.5
Abate-Asdente ^f		13.6
		$\Delta E = 2\delta$ (eV)
Susceptibility, Curie temperature; rectangular band:	Stoner Wohlfarth	0.5
Electronic heat, Curie temperature; rectangular band:	Wohlfarth	1.0
Susceptibility, Curie temperature; experimental $N(E)$ ^g	Shimizu and Katsuki	1.3
Saturation magnetization calculated $N(E)$; (a) as calculated, (b) corrected approximately for electronic heat ^g	Cornwell and Wohlfarth Wohlfarth and Cornwell	(a) 2.7 (b) 1.5
Saturation magnetization; experimental $N(E)$ ^g	Gupta <i>et al.</i> Shimizu and Katsuki	1.5 1.6
Spectroscopic terms; very approximate ^g	Mott	≥ 1.1
$N(E)$ as calculated, saturation magnetization	Abate and Asdente	2.3

^a Reference 4.

^b J. F. Cornwell and E. P. Wohlfarth, *J. Phys. Soc. Japan* **17**, Suppl. B1, 32 (1961). E. P. Wohlfarth and J. F. Cornwell, *Phys. Rev. Letters* **7**, 342 (1961).

^c L. F. Mattheiss, *Phys. Rev.* **134**, A970 (1964).

^d J. Callaway, *Phys. Rev.* **99**, 500 (1955).

^e M. F. Manning, *Phys. Rev.* **63**, 190 (1943).

^f Reference 6.

^g E. P. Wohlfarth, in *Proceedings of the International Conference on Magnetism, Nottingham, 1964* (Institute of Physics and The Physical Society, London, 1965), p. 51.

equivalent \mathbf{k} states in the Brillouin zone. The K_1 value is found positive, in qualitative agreement with the experimental data; from a quantitative point of view the result is less satisfactory; 5.6×10^3 erg/cm³ against the experimental¹³ 5.2×10^5 erg/cm³.

This seems to be a large discrepancy, even for an approximate calculation. This difference may be reduced to a large extent by considering the uncertainty of the parameters involved in the calculation and their influence on the results. For instance, the over-all width of the $3d$ band as evaluated by many authors and the estimated values of the δ parameters reported in Table I can be considered. The values used here perhaps seem too high; a correction by a factor $\frac{1}{2}$, for instance, in the bandwidth and in the δ value produce an increase of K_1 by a factor 8.

The parameter $\bar{\xi}$ can greatly affect the result also. We have here assumed $\bar{\xi} = 354$ cm⁻¹ as obtained by spectroscopic data relative to the ground state of the $3d^7$ ionic configuration, while, for instance, an evaluation relative to $3d^6$ ionic configuration¹² would give $\bar{\xi} = 2460$ cm⁻¹. Thus, a small departure from the assumed $3d^7$ configuration can greatly affect the parameter $\bar{\xi}$, and still more K_1 .

Note added in proof. Besides this fact, some authors [J. R. Anderson and A. V. Gold, Phys. Rev. **139A**, 1459 (1965); R. Braunstein, J. Phys. Chem. Solids **23**, 1423 (1962)] say that the value of the parameter $\bar{\xi}$ for the crystal is considerably greater than the free atom's value.

Moreover, whether it is correct to attribute the same $\bar{\xi}$ to all the states in the crystal is still an open problem, in view of the changing character of the eigenfunctions throughout the band.

2. THE ASPHERICITY OF THE $3d$ ELECTRON DISTRIBUTION

The effect of a cubic field on the atomic fivefold degenerate $3d$ levels is to split them into threefold and twofold degenerate levels: The one of t_{2g} symmetry with atomic functions xy , y^2 , zx , the other e_g with atomic functions $x^2 - y^2$ and $3z^2 - r^2$.

This separation occurs, for example, at the Γ point or at the H point, where the levels are inverted with respect to the ones at Γ (see Fig. 2). The spreading of each level is such that this distinction between t_{2g} and e_g sets does not exist at a general point \mathbf{k} of the Brillouin zone; rather there is a mixing of states, and hence the eigenfunction in general does not possess a net t_{2g} or e_g character. Therefore, it is interesting to consider the charge distribution $q_{e_g}(E)$, $q_{t_{2g}}(E)$ with a definite symmetry as a function of energy; from these curves some data comparable with experimental results by x-ray and neutron diffraction can be deduced.

This distribution has been evaluated from the pre-

TABLE II. Charge and spin distribution for the t_{2g} and e_g symmetries.

	Charge density	Spin density
Present research	66% t_{2g} , 34% e_g	58% t_{2g} , 42% e_g
De Marco and Weiss ^a	70% t_{2g} , 30% e_g	47% t_{2g} , 53% e_g

^a Reference 14.

viously calculated eigenfunctions

$$q_{t_{2g}}(E) = \sum_{E < E_i < E + dE; \tau=1,2,3} |a_{i\tau}|^2,$$

$$q_{e_g}(E) = \sum_{E < E_i < E + dE; \tau=4,5} |a_{i\tau}|^2;$$

dE has been assumed to be equal to bandwidth/100 and is represented in Fig. 3 separately for the t_{2g} and e_g symmetries. At the top and at the bottom of the band the e_g character predominates; however, both kinds of distribution obviously extend all over the bandwidth, and in the high-density-of-states region there are two peaks, more or less marked, with a minimum in the middle of the band. This result is obtained from 385 nonequivalent states in the Brillouin zone.

A weighted spherically symmetric distribution would give 60% t_{2g} and 40% e_g ; the total charge density obtained by x-ray diffraction and the unpaired spin density by neutron diffraction exhibit, on the contrary, a certain asymmetry (see Table II).¹⁴

Some information about both charge and spin densities can be deduced from the curves of Fig. 3 by integrating over all the occupied states and the unpaired spin states, respectively. The result is shown in Table II, the limits of integration $E_{F\downarrow}$ and $E_{F\uparrow}$ being determined from density-of-state curve according to the magnetization data and to the assumed $3d^7$ configuration.

Both the experimental and theoretical results show the same kind of deviation with reference to the spherical symmetry and, as regards the charge distribution, exhibit a good agreement also from a quantitative point of view.

3. THE FERMI SURFACE

In the past few years some measurements have been extended to transition metals which proved to be very powerful in determining the shape of the Fermi surface in normal metals. In particular, there are measurements of the de Haas-van Alphen (dHvA) effect and of magnetoresistance in iron⁸ for which theoretical results would be very interesting.

The form of the Fermi surface has been evaluated

¹³ C. D. Graham, Jr., J. Appl. Phys. **31**, 150S (1960).

¹⁴ J. J. De Marco and R. J. Weiss, Phys. Letters **18**, 92 (1965).

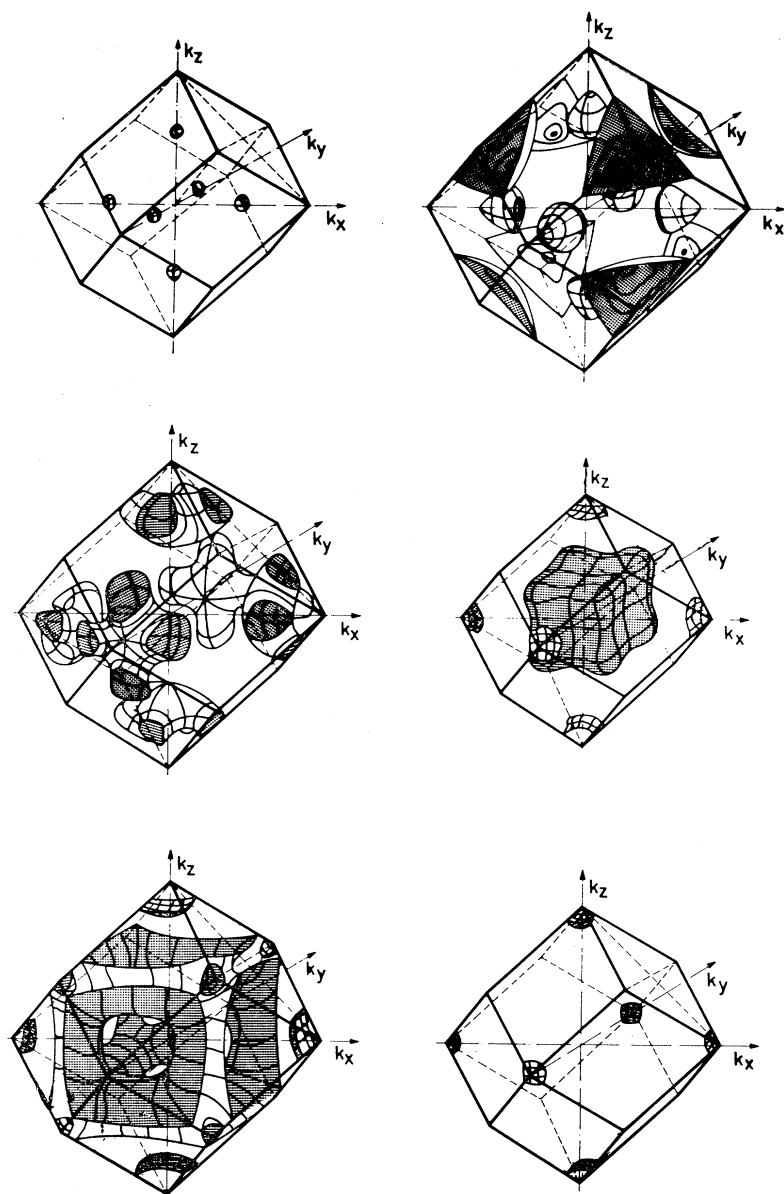


FIG. 5. Spin-down (on the left) and spin-up (on the right) Fermi surfaces for a ferromagnetic state with magnetic moment equal to $\sigma/2$ (σ is the saturation moment). The dark portions of the surfaces are directed towards the occupied states. (The order of the figures relative to the different zones is the same as in Fig. 4).

in the above approximations for the d band only, not including the s - d mixing, and attributing a free-electron Fermi surface to the $4s$ electrons. For each value of the wave vector \mathbf{k} , there are five $E(\mathbf{k})$ values in the d band which have been associated, so that the lowest belongs to the first Brillouin zone, the next highest one to the second Brillouin zone, and so on. As for paramagnetic iron, whose Fermi level has been previously determined (see Fig. 4, Ref. 6), it is found that the highest three zones contribute to the Fermi surface, the different sheets being as represented in Fig. 4. The 3rd and 4th zones give two similar surfaces, while the 5th gives electron pockets on Δ and Σ lines (using the notation of Bouckaert *et al.*¹⁵).

¹⁵ L. P. Bouckaert, R. Smoluchowski, and E. Wigner, Phys. Rev. **50**, 58 (1936).

The d -band $E(\mathbf{k})$ trend is quite different from that of free electrons, and thus the Fermi surface is expected to be greatly affected also by the value of E_F in the band, i.e., by the assumed electron configuration in the metal. In order to test this point, and also to see how the Fermi surface tends to change as the metal is turning ferromagnetic, the Fermi surface for two other values of the energy, the one on the left and the other on the right of the Fermi level just considered, are also determined and represented in Fig. 5. These two levels correspond to spin-down and spin-up Fermi levels in a ferromagnetic state with magnetic moment equal to $\frac{1}{2}\sigma$ (where σ is the saturation moment).

For the complete ferromagnetic state, the spin-down Fermi level is placed near the minimum of the density-of-state curve, and the corresponding Fermi surface

is expected to exhibit the qualitative features of the Cr-group metals; whilst the spin-up Fermi level is placed near the top of the band and, according to this model, the relevant portions of its Fermi surface are expected to consist of hole pockets around H for three bands, and other more or less spherical hole regions around Γ for two bands.

As mentioned above, the Fermi surface is very sensitive to the details of the $E(\mathbf{k})$ curve, and thus to the approximations assumed. The s - d mixing, for instance, certainly induces some modification; but this effect is hard to evaluate, principally because of the uncertainty in the relative positions of the s and d bands, which, as pointed out above, depend critically on the assumed potential. Nevertheless, a comparison between the results obtained by tight-binding and APW cal-

culations^{16,17} in ΓNH plane for the Cr-group transition metals, for instance, shows the same qualitative features of the Fermi surface and suggests that, at least in some regions of the Brillouin zone, even such a simplified model can give some useful suggestions.

ACKNOWLEDGMENTS

The authors are grateful to Professor J. Friedel for his helpful discussion and comments on a preliminary version of this paper. Thanks are due also to Dr. M. Lunelli and collaborators of the Centro Calcolo dell'Università di Milano for their assistance in the numerical computations.

¹⁶ M. Asdente, Phys. Rev. **127**, 1949 (1962).

¹⁷ W. M. Lomer, Proc. Phys. Soc. (London) **80**, 489 (1962); **84**, 327 (1964); T. L. Loucks, Phys. Rev. **139**, A1181 (1965).

Electron-Magnon Interaction in Ferromagnetic Transition Metals*

L. C. DAVIS† AND S. H. LIU

Institute for Atomic Research and Department of Physics, Iowa State University, Ames, Iowa

(Received 4 May 1967)

The self-energy of an electron in a ferromagnetic transition metal due to the virtual emission and absorption of magnons has been calculated. It was found that the mass correction due to the electron-magnon interaction may be as large as that due to the electron-phonon interaction. Furthermore, it was noted that singularities in the density of states should occur at $\epsilon_F \pm \hbar\omega_0$, where ω_0 is the frequency of the magnon emitted or absorbed when electrons or holes forward-scatter from the Fermi surface of one spin band to the other spin band.

EXPERIMENTAL studies of the ferromagnetic transition metals may soon indicate the extent to which the electron mass at the Fermi surface is renormalized by the electron-magnon interaction.^{1,2} The purpose of this paper is to report some results of a theoretical calculation of this mass correction and other effects associated with the self-energy of an electron due to the virtual emission and absorption of magnons.

We take the interaction Hamiltonian in second quantized form to be

$$H_{\text{int}} = J\Omega_0 \int d^3r \mathbf{s}(\mathbf{r}) \cdot \mathbf{S}(\mathbf{r}), \quad (1)$$

where $\mathbf{s}(\mathbf{r}) = \frac{1}{2}\psi^\dagger(\mathbf{r})\boldsymbol{\sigma}\psi(\mathbf{r})$ [$\psi(\mathbf{r})$ is the electron field operator and σ_i is a Pauli spin matrix, $\hbar=1$] and $\mathbf{S}(\mathbf{r})$ is the net spin polarization per unit volume. The

exchange constant is J , and Ω_0 is the volume of a unit cell. We introduce magnon creation and annihilation operators in a fashion similar to Kittel's³:

$$S^+(\mathbf{r}) = \left[\frac{2}{\Omega} \left(\frac{S}{\Omega_0} \right) \right]^{1/2} \sum_{\mathbf{q}} e^{-i\mathbf{q}\cdot\mathbf{r}} b_{\mathbf{q}},$$

$$S^-(\mathbf{r}) = \left[\frac{2}{\Omega} \left(\frac{S}{\Omega_0} \right) \right]^{1/2} \sum_{\mathbf{q}} e^{i\mathbf{q}\cdot\mathbf{r}} b_{\mathbf{q}}^\dagger, \quad (2)$$

and

$$S_z(\mathbf{r}) = \frac{S}{\Omega_0} - \Omega^{-1} \sum_{\mathbf{q}, \mathbf{q}'} e^{i(\mathbf{q}-\mathbf{q}')\cdot\mathbf{r}} b_{\mathbf{q}}^\dagger b_{\mathbf{q}'},$$

(Ω is the volume of the crystal.) In the ground state, $S_z(\mathbf{r}) = S/\Omega_0$, where S is the net spin polarization per atom.

The electron energies are $\epsilon_\sigma(\mathbf{k}) = \epsilon(\mathbf{k}) + (\sigma/2)JS$, so that the exchange splitting is JS . We assume that the magnon or spin-wave frequencies $\omega(\mathbf{q})$ are known.

* Work was performed in the Ames Laboratory of the U.S. Atomic Energy Commission. Contribution No. 2083.

† Atomic Energy Commission postdoctoral fellow.

¹ A. C. Joseph and A. C. Thorsen, Phys. Rev. Letters **11**, 554 (1963).

² D. C. Tsui and R. W. Stark, Phys. Rev. Letters **17**, 871 (1966).

³ C. Kittel, *Quantum Theory of Solids* (John Wiley & Sons, Inc., New York, 1963).